Int J Adv Manuf Technol (2015) 78:1393–1405
DOI 10.1007/s00170-014-6747-x

ORIGINAL ARTICLE

Finite element modeling of hard turning process via a micro-textured tool

Dong Min Kim · Vivek Bajpai · Bo Hyun Kim · Hyung Wook Park

Received: 8 February 2014 / Accepted: 19 December 2014 / Published online: 9 January 2015

Abstract Literature survey showed that the micro-textures on the tool rake face can help in reduction in friction at chip-tool interface and therefore, reduction in the cutting forces. Consequently, the current work is based on FE simulation of hard turning of bearing steel (AISI52100). Four types of micro-textures have been considered on the tool rake face: non-texture, perpendicular, parallel, and rectangle. Johnson-Cook (J-C) material constitutive law has been considered for the workpiece with temperature-dependent material properties. Experimental work has been performed at cutting conditions: type, parallel; edge distance, 0.195 mm; pitch size, 0.110 mm; and height of the texture, 0.049 mm to validate the current machining model. Parametric study of effect of tool feature parameters on the cutting forces has been performed. Based on the current model, it is observed that the perpendicular shape showed the minimum cutting force. The maximum reduction of 28 % was predicted in the effective coefficient of friction compared to the non-textured surface. Additionally, effect of size of the texture (edge distance, pitch size, texture height) and the friction factor at tool-chip interface on the process responses is predicted. The perpendicular texture at an edge distance of 100 μm, pitch size of 100 μm, and texture height of 50 μm showed the most effective shape and size for the minimum cutting forces and effective friction. It is simulated that the chip flow angle can be governed by the shape/size of the texture on the tool rake face. It is expected that the current model can further be helpful in the characterization of other hard materials and complex texture shape/size.

Keywords Hard turning · Textured tool · FEM · Machining · Hard cutting

D. M. Kim · V. Bajpai · H. W. Park (✉)
Department of Mechanical Engineering, Ulsan National Institute of Science and Technology, UNIST-gil 50, Eonyang-eup, Ulju-gun, Ulsan 689-798, Republic of Korea
e-mail: hwpark@unist.ac.kr

B. H. Kim
Department of Mechanical Engineering, Soongsil University, Sangdo-Ro 369, Dongjak-Gu, Seoul 156-743, Republic of Korea

1 Introduction

Hard turning is a machining process, which increases productivity by eliminating unnecessary machining steps and improving the material removal rate [1]. Hard turning is used to machine difficult-to-cut materials like hardened steel (50–70 HRC) at high cutting speed with a single-point contact method. Cubic boron nitride (CBN), ceramics, and cermet are the commonly used tool materials [2]. Two varieties of CBN materials are commercially available: high CBN content (90 %) and low CBN content (50–70 %) [3]. Hard turning has particular advantages when manufacturing engines, bearings, and precision components with levels of roughness as low as Ra (<500 nm) without grinding. The rate of material removal is higher in hard turning than grinding machining [4]. However, the cutting temperature can reach more than 900 C [5]. The white layer generated on the machined surface of the workpiece increases its surface residual stress [6]. High friction is the most severe problem in the hard turning process; it increases temperature, which reduces tool life significantly [6]. Therefore, reducing the friction between the tool and the workpiece is extremely important in improving the process. It is reported that the friction between the tool-chip interface and the cutting forces can be reduced via micro-textured surface on the tool rake face [7–10]. Macro-sized textures increase friction; however, micron-ordered textured surface reduces

Table 1 Material constants of the J-C flow stress model for AISI52100 bearing steel [23]

A [MPa]	B [MPa]	*n*	*C*	*m*	Tmelt (°C)
774.78	134.46	0.371	0.0173	3.171	1487

friction and improves lubrication. Smaller texture sizes reduce friction because the debris from wear becomes entrapped in the texture geometry [11, 12] and increases lubrication in the tool-chip interface [13–15]. Additionally, the decrease in the contact area between the tool rake and the chip surface decreases the frictional force [16]. Textured tools have been developed and used for machining, and it is reported that the textured surface on the tool rake face decreases the cutting force due to reduction in the friction by reducing the contact length in the tool-chip interface. [17–19] Simulated dry cutting with a textured rake face on carbide tools showed the effect of textured surfaces and solid lubricant on the von Mises stress and cutting force [19]. However, the work has not been considered by the point of view for the interfacial textured tool and the workpiece. This type of problem has been considered to be an important subject of research. Machining simulation of textured tool has not been reported.

Consequently, the aim of the current work is to simulate hard turning with textured tool. Johnson-Cook (J-C) material model has been implemented on the workpiece. Further, the model is used to study effect of the shape and size of the texture on the cutting forces, effective friction between chip and the tool rake face, and the chip flow direction.

2 Finite element modeling

Deform 3D commercial finite element codes have been used in the modeling of the hard turning process. The tool has been considered as a deformable body. The current modeling

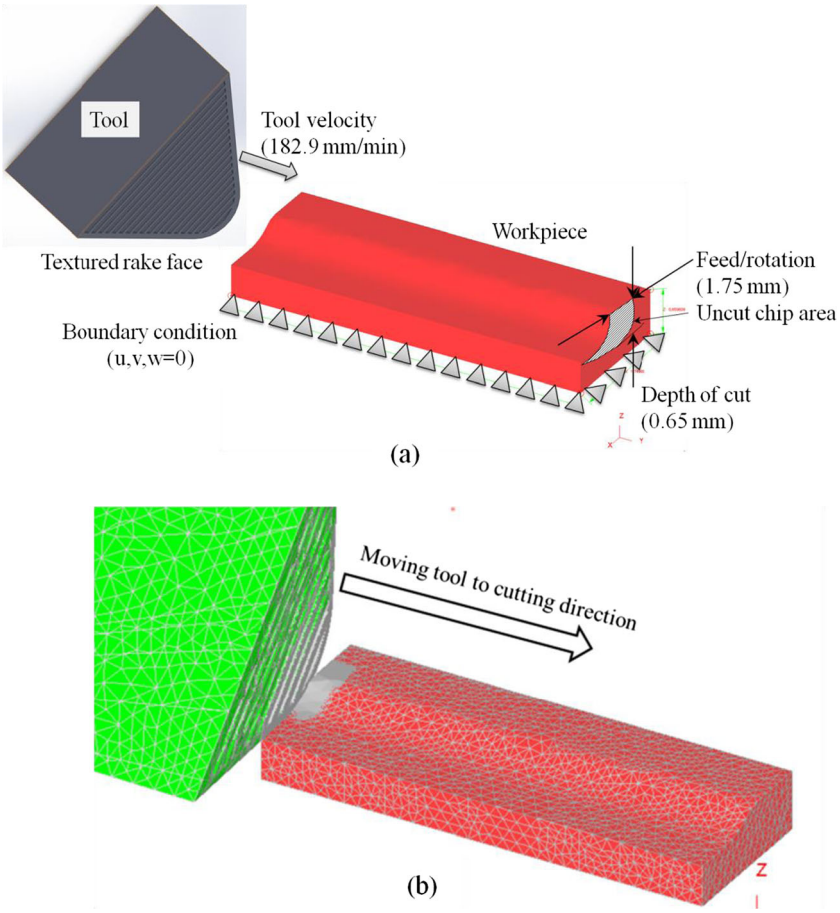

Fig. 1 **a** Model assembly and boundary conditions. **b** mesh

process contains two major modules: numerical formulation of the problem and the chip formation mechanism. The numerical formulation contains geometrical modeling, interaction between the tool face and the workpiece, loading and boundary conditions, and material properties. The J-C material model has been adopted to define the material's plasticity behavior during the machining. The model is further used in parametric study of process parameters on machining response like cutting forces, effective coefficient of friction, and chip flow angle.

2.1 Workpiece material model

The J-C material model [20, 21] has been adopted as a material constitutive model (Eq 1.). The J-C model has been implemented because of its capability of large strain and strain rates. Equivalent stress can be express in the J-C model as:

$$\overline{\sigma} = \left[A + B\cdot\overline{\varepsilon}^{\,n}\right]\cdot\left[1 + C\cdot\ln\left(\frac{\overline{\varepsilon}}{\overline{\varepsilon}_0}\right)\right]\cdot\left[1-\left(\frac{T-T_{\text{room}}}{T_{\text{melt}}-T_{\text{room}}}\right)^{m}\right] \tag{1}$$

where A is the yield stress, B is the strain hardening coefficient, n is the strain hardening exponent, C is the strain rate dependence coefficient, and m is the temperature dependence coefficient. $\overline{\varepsilon}$ is the equivalent plastic strain rate. $\overline{\varepsilon}_0$ is the reference strain rate. T_{melt} is the melting temperature for the material (Table 1).

2.2 Numerical formulation

The commercial software Deform 3D® has been used to model the cutting process. A 3D turning model was developed to simulate the cutting forces and chip formation (see Fig. 1). A rotating workpiece has been transformed to a linear machining condition to provide simplicity in simulation. The outer surface of the workpiece was fixed in all three linear directions and a sink temperature of 20 C was applied on it. The tool was set at the feed velocity (182.9 mm/min) towards the workpiece. A tetrahedral thermally coupled 38,000 elements have been used in the workpiece. A similar element type has been used in the tool with 138,000 elements. The initial temperature of the tool and workpiece was kept at 20 C. An air convection of 0.02 N/s/mm/°C has been applied on the free surface and the heat transfer coefficient has been set at 28 N/s/mm/°C (Table 2).

Table 2 Physical properties of AISI52100 steel (62HRC) [5, 24, 25]

Properties	Value	
Density, ρ [kg/m3]	7853	
Elastic modulus, E [MPa]	Value [MPa]	Temperature [K]
	201,330	293.15
	178,580	473.15
	162,720	673.15
	103,420	873.15
	86,870	1073.15
	66,880	1273.15
Poisson's ratio, ν	Value	Temperature [K]
	0.277	293.15
	0.269	473.15
	0.255	673.15
	0.342	873.15
	0.396	1073.15
	0.49	1273.15
Thermal conductivity	Value [W/mK]	Temperature [K]
	52.5	293.15
	47.5	473.15
	41.5	673.15
	32.5	873.15
	26	1073.15
	29	1273.15
	30	1473.15
	29.5	1573.15
Expansion coefficient, α (μm/m/K)	Value $\times 10^{-5}$ [m]	Temperature [K]
	1.19	293.15
	1.25	373.15
	1.3	347.15
	1.36	573.15
	1.41	673.15
	1.45	773.15
	1.49	873.15
	1.49	1773.15
Tmelt (K)	1760.15	
Heat capacity	Value [N/mm2oC]	Temperature [K]
	3.354	293.15
	4.0622	473.15
	4.75	673.15
	5.75	873.15
	6.0278	973.15
	12.75	1023.15
	5	1073.15
	4.5	1173.15

Table 3 Tool geometry specification used in the simulations [4] and material properties [3, 4, 26, 27]

Tool geometry		Low CBN tool material properties	
Tool geometry specification	Value	Properties	Value
Nose radius, $r\varepsilon$	0.8 mm	Young's modulus (Gpa)	588
Side rake angle, $\gamma 0$	−5°	Poisson's ratio	0.17
Back rake angle, χs	−5°	Thermal expansion ($\times 10^{-6}$/°C)	0.47
Side cutting angle, λc	−5	Emissivity [23]	0.45
		Thermal conductivity (N/s/°C)	f(T)
		Heat capacity (N/mm2/°C)	f(T)

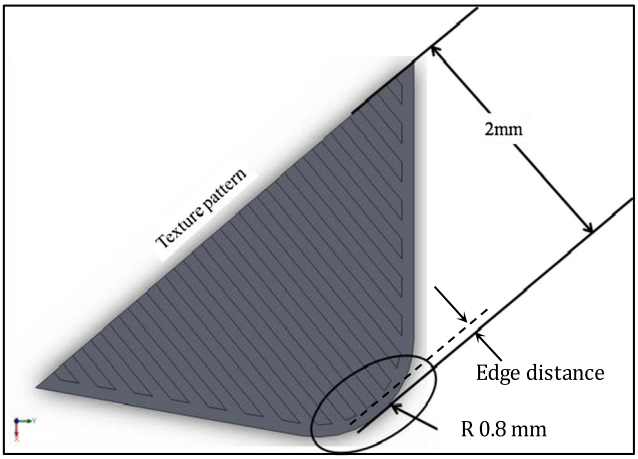

Fig. 2 Tool geometry with the pattern

2.3 Tool geometry and properties

A tool tip was designed based on the geometry listed in Table 3. The length of the tool tip was kept at 2 mm to facilitate chip flow on it. Temperature-dependent material properties have been considered in the simulation. Temperature-dependent thermal conductivity and heat capacity of the tool material are listed in Table 4. Figure 2 shows magnified view of tool geometry. A textured rake face shows edge distance and tool nose radius.

2.4 Simulation conditions

The four geometric shapes that have been considered in the simulation are texture shape, edge distance, pitch size, and texture height. Size of the textures has been expressed in edge distance, pitch size, and texture height. Three levels of edge distance and pitch size and two levels of texture height have been considered. In addition of the shape and size of the texture, the friction of coefficient between the chip and tool has also been varied at three levels. Table 5 shows levels of all four geometric shapes, size, and the tool-chip friction coefficient. Figure 3 shows geometry of four types of textures viz.: (a) flat (non-textured surface), (b) perpendicular (ridges, perpendicular to the chip flow direction), (c) parallel (ridges, parallel to the chip flow direction), and (d) rectangular: This is a combination of both parallel and perpendicular textures; array of pillars have been fabricated by cross cutting of the tool face. The cutting parameters were selected from a previously reported work [3]: cutting speed of 182.9 mm/min, feed rate of 0.152 mm/rev, and depth of cut of 0.203 mm.

Five cases of process parameters were selected for the simulation. The first case was performed with the four types of textures at 100 μm of edge distance, 100 μm of pitch size, 50 μm of height of the texture, and a shear friction of 0.6. Based on the cutting forces, the perpendicular textures were selected as the optimum shape of the texture. The next cases were considered for the perpendicular texture. The edge distance was considered as the varying parameters

Table 4 Thermal properties of the tool material [23, 24]

Temperature (°C)	Thermal conductivity (N/s/°C)	Heat capacity (N/mm2/°C)
20	59.4	2.7
100	64.4	3.3
200	67.7	4.0
400	68.8	4.7
600	66.7	5.1
800	63.9	5.3
900	62	5.4
1000	59.5	5.4

Table 5 Simulation parameters for the patterned insert

Process parameter	Texture	Edge distance	Pitch size	Texture height	Shear friction
Level 1	Flat	50	50	50	0.2
Level 2	Perpendicular	100	100	100	0.4
Level 3	Parallel	150	150	–	0.6
Level 4	Rectangular	–	–	–	–

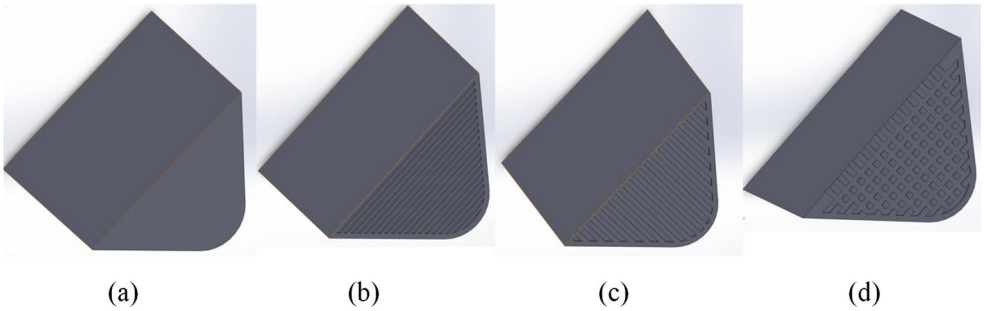

Fig. 3 Textured tool insert. **a** non-textured. **b** perpendicular. **c** parallel. **d** rectangular

with the constant pitch size of 100 μm and a height of the texture at 50 μm with a friction coefficient of 0.6 in case 2. Case 3 considered the pitch size as the varying process parameter by keeping other parameters constant. Case 4 and 5 have considered feature size and the friction coefficient as varying process parameters, respectively. Table 6 shows the combination of process parameters, used in each run of simulation.

Table 6 Simulation parameters related to tool geometry

Case no.	Parameter	Variable	Fixed	
1	Texture shape	Non-textured	Edge distance (μm)	100
		Perpendicular	Pitch size (μm)	100
		Parallel	Height (μm)	50
		Rectangular	Friction	0.6
2	Edge distance (μm)	50/100/150	Texture shape	Perpendicular
			Pitch size (μm)	100
			Height (μm)	50
			Friction	0.6
3	Pitch size (μm)	50/100/150	Texture shape	Perpendicular
			Pitch size (μm)	100
			Height (μm)	50
			Friction	0.6
4	Texture height (μm)	50/100	Texture shape	Perpendicular
			Edge distance (μm)	100
			Pitch size (μm)	100
			Friction	0.6
5	Shear friction	0.2/0.6/0.8	Texture shape	Perpendicular
			Edge distance (μm)	100
			Pitch size (μm)	100
			Height (μm)	50

3 Model validation

Experimental works have been performed to validate the present machining model. Turning operation was performed with a parallel-textured tool with a cutting speed at 182.0 m/min, feed at 0.152 mm/rev, and a depth of cut at 0.203 mm. The experiments were performed on a turning machine (TSL-6, S&T Dynamics, Korea). Figure 4 shows the experimental setup and the micro-textured tool for the hard turning process. The cutting forces were measured on a three component dynamometer (Kistler 9257B, Switzerland). The tool was prepared by electro-discharge machining (EDM). The tool geometry is: type, parallel; edge distance, 0.195 mm; pitch size, 0.110 mm; and height of the texture, 0.049 mm. Figure 5 shows comparison of cutting forces from simulation and the experimental work. It is observed that the model is well capturing the cutting force with an error in prediction of 7.5 %. The error in the prediction in the thrust force is 70 %, which shows irrelevant prediction. The error in the prediction

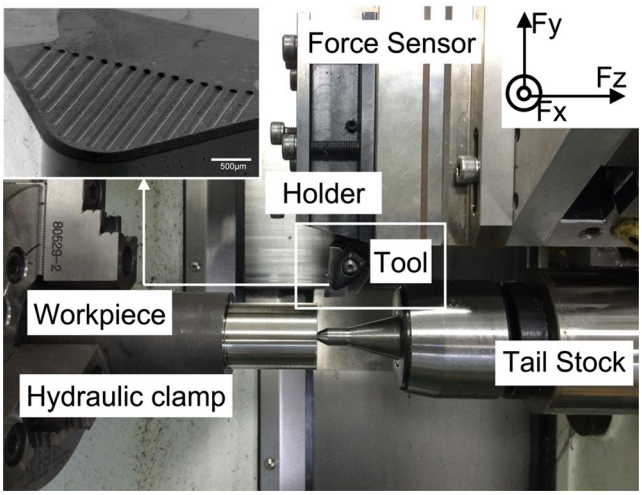

Fig. 4 Experiment setup of the hard turning with micro-textured tool and a SEM image of the parallel texture on the tool rake surface

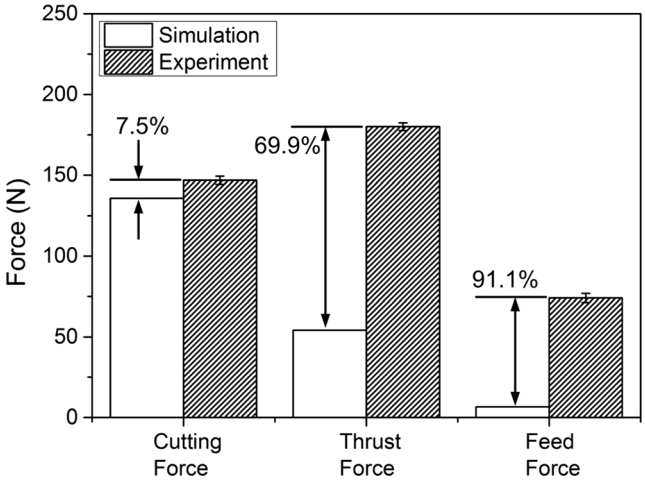

Fig. 5 Comparison between experimental results and predictions with the parallel-textured insert

is higher due to the assumptions in the simulation. The simulation considered a sharp cutting tool, whereas there is a finite size of the nose radius present during the experimental work. Similarly, the simulation is not predicting the feed force due to the same assumption of the tool nose radius. The cutting force is the important component of the forces, which is responsible in the design of the tool shank and is responsible for the tool wear and the catastrophic failure of the tool. Therefore, the prediction of the cutting force is sufficient for the model.

4 Results and discussion

Effect of the feature geometry (shape, edge distance, pitch size, height) and the shear friction have been studied on the cutting forces (cutting, thrust, feed direction), the effective friction coefficient, and the chip flow angle. The cutting force is the most important force than the feed force and the thrust force. It is observed that the cutting force varied between 100 and 150 N, whereas, the feed and the thrust force are limited to 70 N. Therefore, in most of the analysis, only the effect of process parameter on the cutting force has been analyzed. The effective coefficients of friction were found lower than the set value with the patterned tool.

4.1 Effect of texture shape

Case no.1 from Table 1 has been considered for the study of the effect of the shape of the texture on the machining response. The effect of the textures on the cutting forces and the effective friction coefficient were performed at an edge distance of 100 μm, pitch size of 100 μm, height of the texture at 50 μm, and a shear friction of 0.6. Figure 6 showed that the force in the cutting direction is the maximum in all type of forces and it is least with the perpendicular texture shape. Six percent reduction in the cutting force has been predicted in the perpendicular texture than the flat tool. The thrust direction force is again minimized for the perpendicular texture. The only force in the feed direction is maximized with perpendicular texture. The amount of the feed direction force is very less; therefore, it can be neglected.

From Fig. 6, it is clear that the effective coefficient of friction (cutting/thrust force) was lowest for the perpendicular and parallel texture. However, the lowest cutting and thrust force occurred with the perpendicular texture. The largest friction occurred for the flat (non-texture), as shown in Fig. 6. All of the textures showed similar behavior as to reduce the friction than the flat textured tool. Based on the cutting force data and the effective coefficient of friction, it can be stated that the perpendicular texture is the best shape of the texture, which can be studied further with the variation in the size. Twenty-five percent reduced friction coefficient has been predicted with the perpendicular texture than the flat non-textured surface. The similar results have also been suggested by other researchers [9, 22].

The chip was subjected at higher stress after the pitch position (see Figs. 7a to d). The parallel and rectangular textures clearly concentrated the stress on the pattern position. The texture of the rake face governed the chip flow direction based on the shape of the texture. The flat and rectangular textures showed the chip flow angles of 75–76°. The perpendicular texture had the smallest chip flow angle of 44°, the chip is following in the pattern direction towards the unmachined area of the workpiece. The parallel texture had a 90° chip flow angle, due to the rotation of the chip in the direction of the parallel pattern. Thus, the perpendicular texture had the effect of decreasing the cutting force by curling the chip away from the rake face. This can be attributed as the similar effect of oblique cutting than the orthogonal cutting. A close control on chip flow direction can help in effective chip removal from the machining zone and can further help in designing an automated process.

4.2 Effect of edge distance

The simulation conditions of case no. 2 in Table 6 have been considered for the study of the edge distance on the cutting forces, effective coefficient of friction, and the chip flow angle. Figure 8a showed that the cutting force decreases by

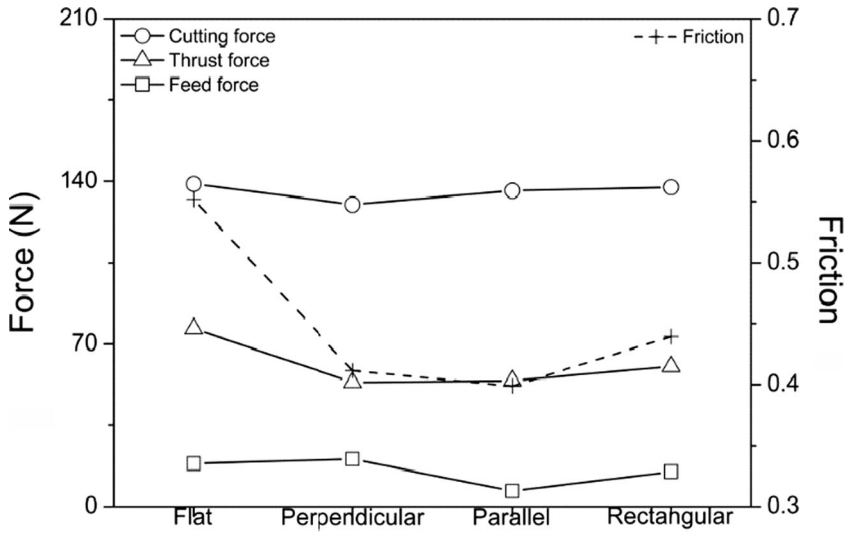

Fig. 6 Predictive force and friction factor of various texture shapes

30 % if the edge distance changes from 50 to 100 μm. Further increase in the edge distance increases the cutting force by a small amount. A 7 % increase in the cutting forces was predicted if the edge distance changes to 150 μm. Cutting force data showed no change in the cutting force if the edge distance changes to 200 μm. It showed that the cutting force was minimum at an edge distance of 100 μm which agreed with the previously reported work [22]. The smaller edge distance prevents the chip separation and therefore the predicted cutting force was higher. As the edge distance increases, the secondary shear zone shifts to the region of the textured and non-textured surface which again increases the cutting force. The value of edge distance of 100 μm can be considered as the optimum value for keeping the secondary shear zone on the textured surface and provide chip separation. Similar to the cutting force, thrust force showed the similar trend except the maximum edge distance of 300 μm. The feed force is maximum with the 100 μm edge distance; it can be ignored due to the low value of the feed force. The effective friction coefficient is found minimum at 300 μm edge distance.

Figure 9a–d shows the effect of the edge distance on the chip flow angle. The predicted chip angle varies from 116° at the edge distance of 50 μm to 44° at the edge distance of 100 μm. The decrease in the chip angle supports the chip to escape out from the rake face. Further, the chip angle increases to 55° if edge distance changes to 150 μm. The maximum edge distance of 300 μm showed the chip angle at 49°. It means further increases in the edge distance results in minimization of the chip rotation angle due to the shifting of the secondary shear zone into the transition line between the textured and the plane surface.

4.3 Effect of pitch size

Case no.3 in Table 6 has been simulated to analyze the effect of the pitch size on the cutting forces, effective coefficient of friction and chip flow angle on the perpendicular texture at 100 μm edge distance, 50 μm feature height, and 0.6 shear friction coefficient. Figure 10 shows variation of cutting force and friction coefficient with the pitch size. It is predicted that the cutting force decreases if the pitch size increases from 50 to 100 μm by 33 %. Further increase in the pitch size increases the cutting force by 36 %. In addition of the cutting force, the feed force and the thrust force are minimized at the pitch size of 100 μm. However, the experimental results [9, 22] indicated that the force diminished as the pitch size increased linearly. This was due to the different size effects in the experiments. The effective coefficient of friction is almost stable with the change in the pitch size. In the experiments [22], the friction coefficient in the cutting direction increased as the pitch size increased. A negligible increase in the coefficient of friction has been shown by the predicted force in Fig. 10. The chip flow angle is shown in Fig. 11. The chip flow angle is a maximum of 44° for the pitch size of 100 μm. The chip flow angle changes to 30° if the pitch size changes to 150 μm. The chip flow angle was acquired at 26° if the pitch size was 50 μm. Therefore, it can be concluded that the fine texture can bend the chip more effectively due to

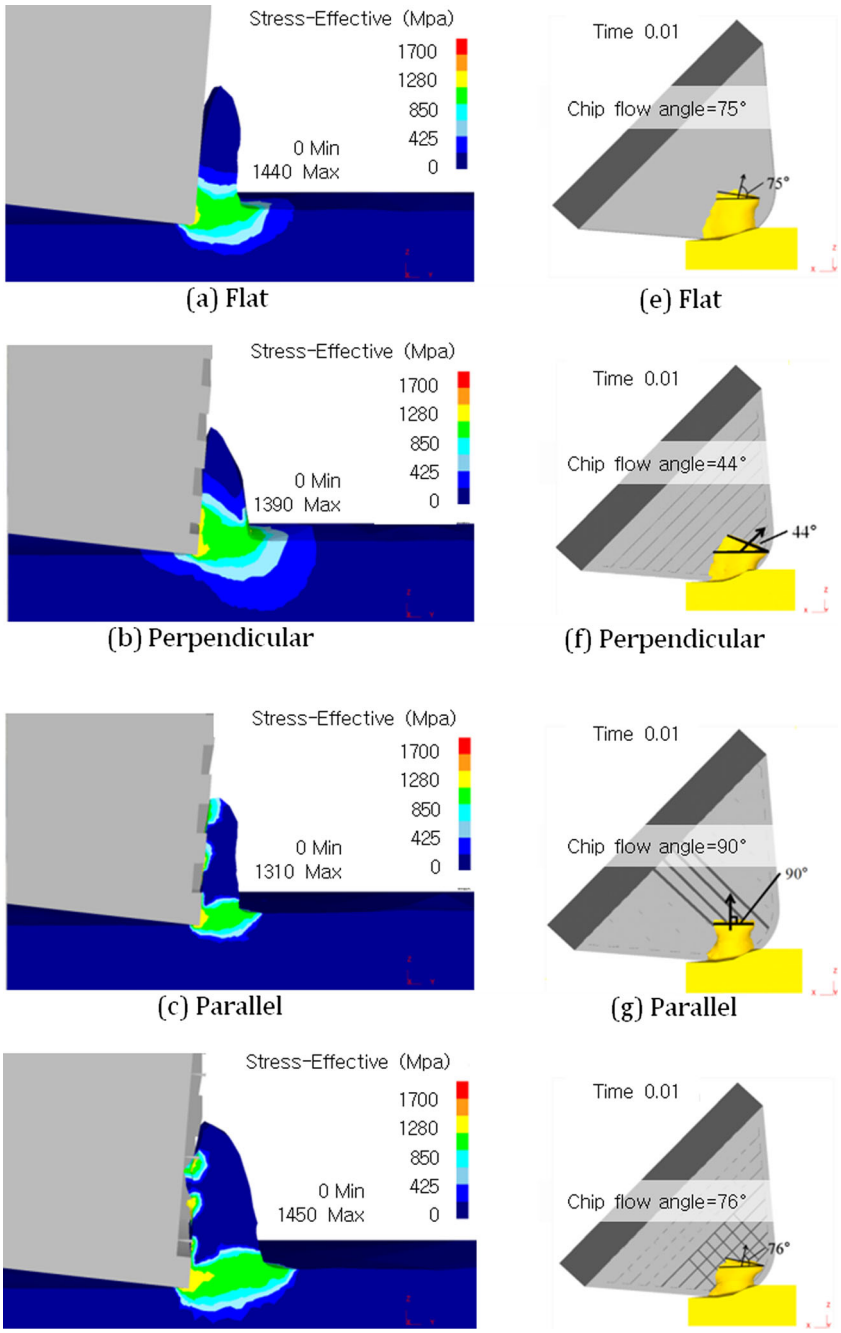

Fig. 7 **a**–**d** Effective stress on the tool-workpiece cross-section. **e**–**h** chip flow angle

gripping the deformed material over the channels of the texture.

4.4 Effect of texture height

Figure 12 shows the predictive forces and the effective coefficient of friction for texture heights of 50 and 100 μm (case no. 4 in Table. 6) on perpendicular features at edge distance of 100 μm, pitch size of 100 μm, and a friction coefficient of 0.6. It is predicted that the cutting force is increased by 23 % if the height of the pattern increases from 50 to 100 μm. The thrust and the feed forces show almost flat response and no change with the change in the pattern height. Increase in the height showed a little decrease in the effective coefficient of friction.

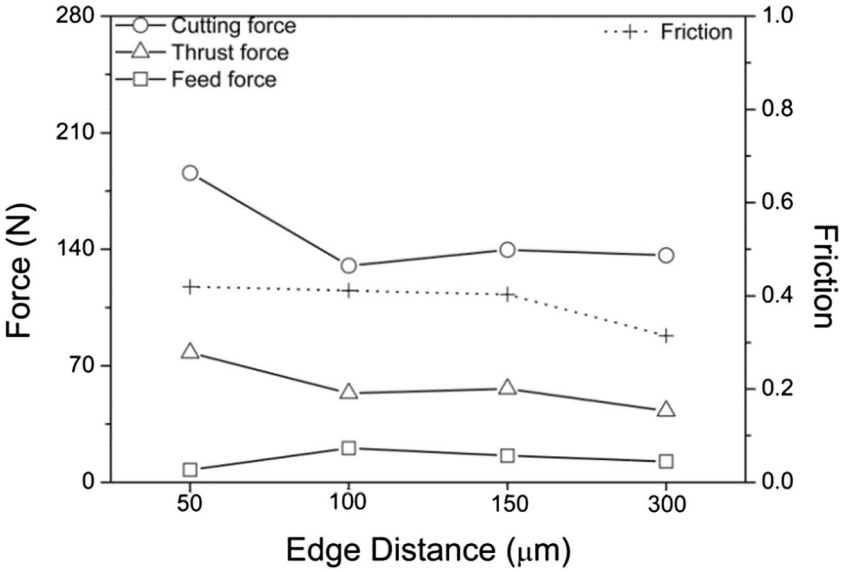

Fig. 8 Curling of the chip at edge distance of **a** 50, **b** 100, **c** 150, and **d** 300 μm

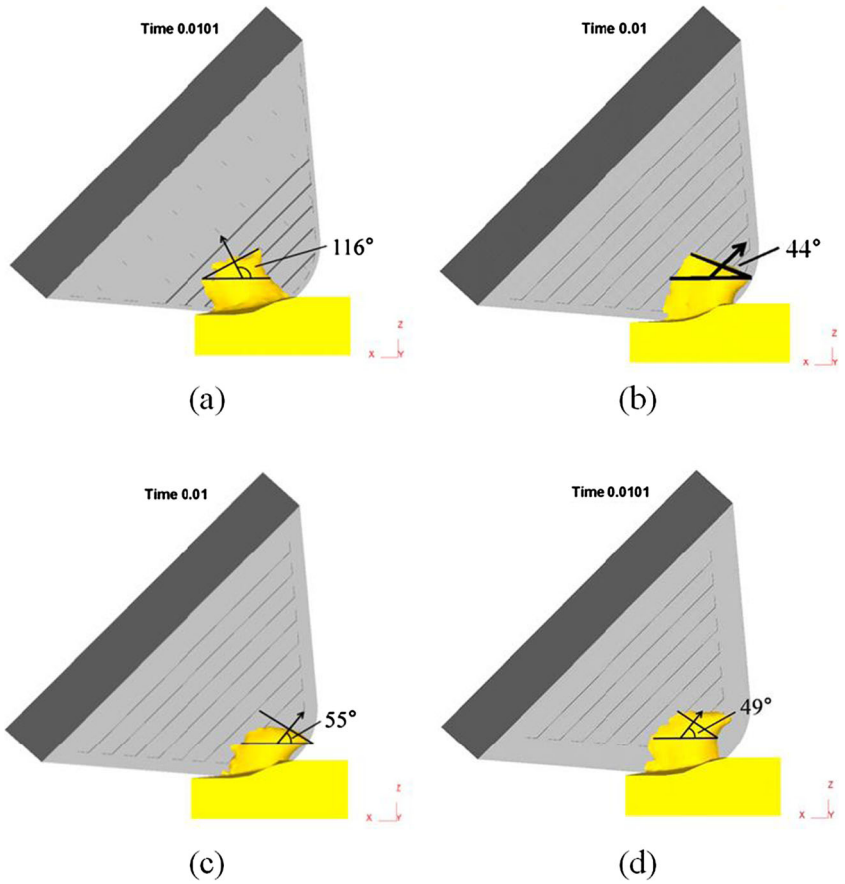

Fig. 9 Predictive force and friction for the perpendicular pattern as a function of edge distance

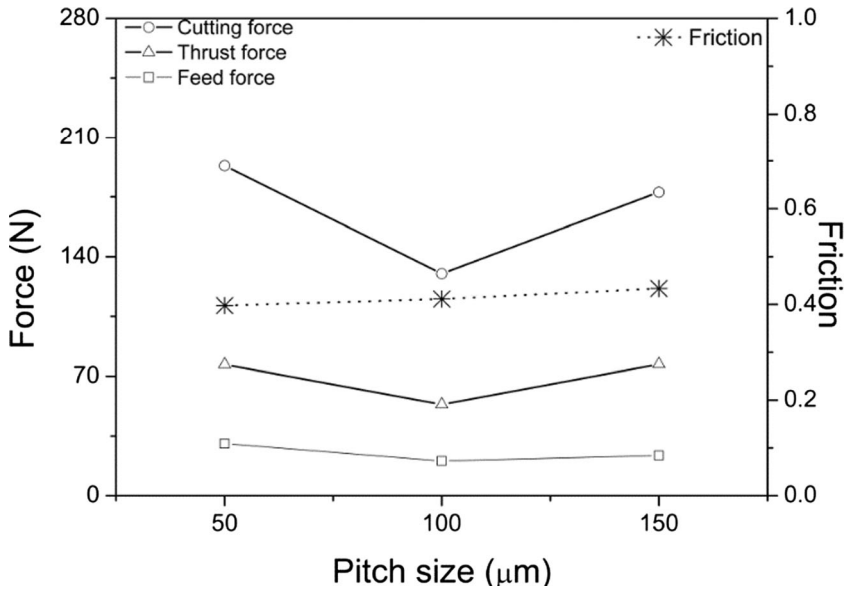

Fig. 10 Effect of pitch size on the predictive force and friction

The experimental results [9, 22] showed the opposite tendency: The measured force decreased as the height increased. However, the height range in the simulation is greater than the experiments. The pattern height in the experiments was less than 10 μm. The chip flow angle decreases if the height of the textures increases to 100 μm (see Fig. 13). The chip bending ability increases with increase in the height of the texture. Therefore, effectiveness of the texture increases with the height.

4.5 Effect of friction factor

Simulations are performed based on the case no. 5 in Table 6. Three levels of shear friction have been considered at and edge distance of 100 μm, pitch size of 100 μm, and a texture height of 50 μm on perpendicular texture. Figure 14 shows effect of shear friction on the cutting forces. Increase in the shear friction from 0.2 to 0.4 does not show any effect of cutting force; however, additional increase to 0.6 shows a reduction of 22 % in the main cutting force. The thrust force is limited to 53.5 N, whereas the feed force is limited to 31 N, which is much lesser than the value of the cutting force. The minimum value of the cutting force is about 130 N at the highest friction coefficient of 0.6. The friction force applied on the rake face has a component in the direction opposite to the cutting force. If the coefficient of friction increases, it increases the component of the friction force in the opposite direction of the cutting force due to negative rake angle. Therefore, increase in the friction coefficient showed reduction in the main cutting force. The effective coefficient of friction is directly related to the shear friction coefficient. It increases from 0.26 to 0.41 if the shear friction coefficient changes from 0.2 to 0.6. It shows that the texture support to the lower friction coefficient but reduces the maximum shear friction coefficient. Increase in the friction

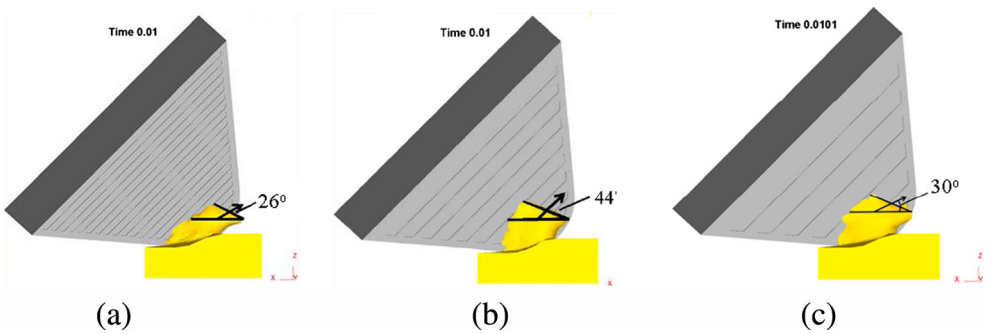

Fig. 11 Chip flow angle at a pitch size of **a** 50, **b** 100, and **c** 150 μm

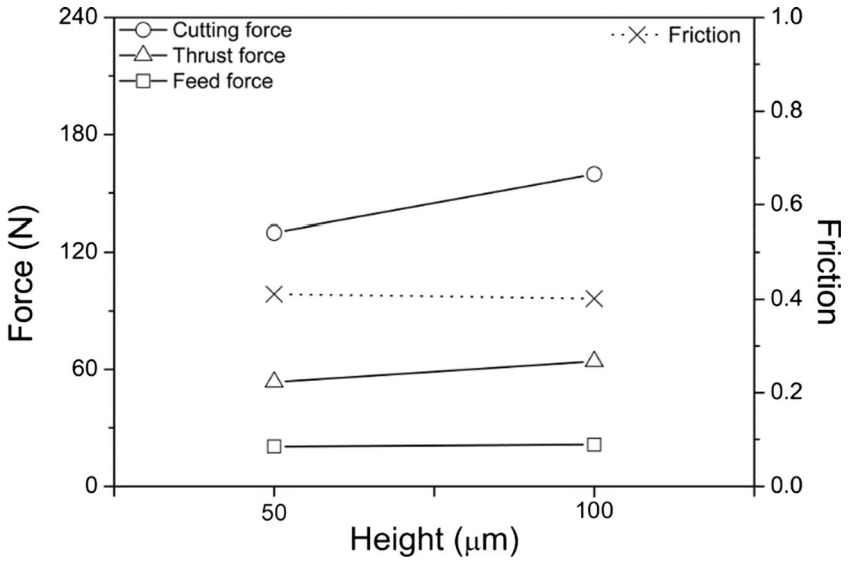

Fig. 12 Effect of height on the predictive force and friction

coefficient increases the frictional force on the chip; therefore, increase in the shear friction showed more bending of the chip and a lower chip flow angle. The lowest coefficient of friction showed a chip flow angle of 52° and the maximum coefficient of friction showed a minimum chip flow angle of 44° (Fig. 15).

5 Conclusions

The current work reported the effectiveness of the tool texturing in hard turning process. The effect of textured tool on cutting forces, effective friction coefficient, and chip flow angle has been simulated by Deform 3D® for hard turning. A turning operation was simulated with the tool having flat non-textured rake face and three different kinds of textures (perpendicular, parallel, and rectangle shape). An experiment was conducted for the validation of the simulation. The cutting force obtained from the experimental work showed that the simulation is well capturing the cutting force. However, this model is not capturing the trust and the feed force due to the tool nose radius. It was observed that the predicted cutting forces and effective friction were decreased with the perpendicular-type texture. A 6 % reduction in the main cutting force and 25 % reduction in the effective friction were predicted with perpendicular texture compared to a non-textured flat tool. The maximum reduction of 28 % in the effective friction coefficient has been predicted with parallel texture.

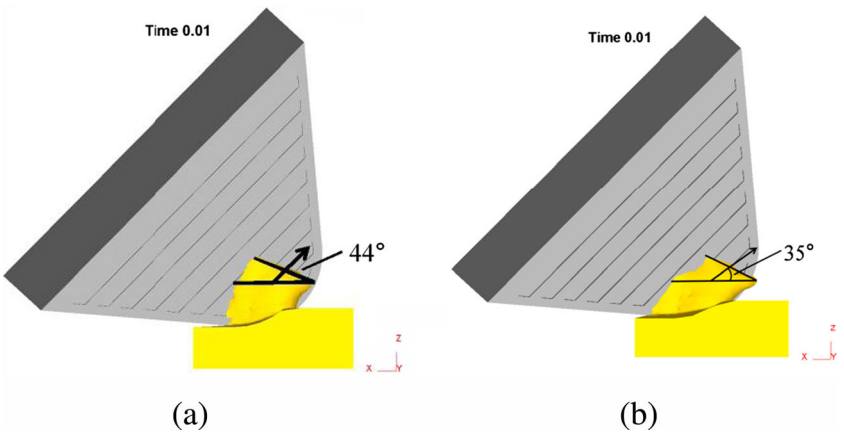

Fig. 13 Effect of texture height on the chip flow angle at **a** 50 and **b** 100 μm

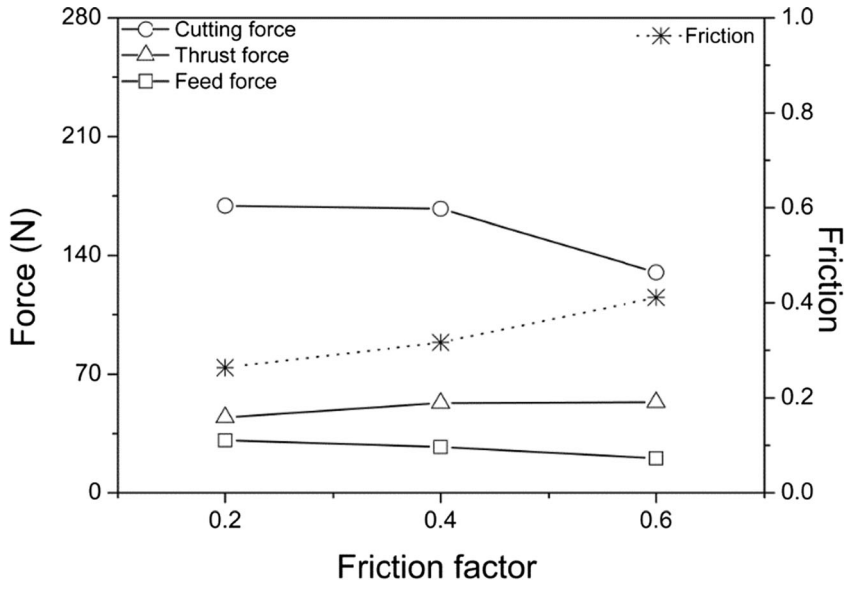

Fig. 14 Effect of friction factor on the predictive force

Further, dimensions of the texture were varied to analyze the effect of the size of the texture on the cutting force, effective friction coefficient, and the chip flow angle. Edge distance, pitch size, and height of the texture were considered as texture dimension. Additionally, friction factor at the tool-chip interface was varied to show the effect on the cutting force and the chip flow angle. Thirty percent lower cutting force was predicted with 100 μm edge distance than a shorter edge distance of 50 μm. Pitch size effect showed a 33 % reduction in the main cutting force if pitch size changes from 50 to 100 μm. Eighteen percent reduction in the main cutting force has been predicted if the height of the texture is reduced from 100 to 50 μm. Cutting force was decreased by 22 % at a friction factor of 0.6 than in the other two conditions. Variation in friction factor from 0.2 to 0.4 has negligible effect on the cutting force. An edge distance of 100 μm, pitch size of 100 μm, texture height of 50 μm, and friction factor of 0.6 showed the minimum cutting force. An edge distance of 300 μm showed the minimum effective friction coefficient at tool-chip interface. A natural chip flow angle of 75° has been predicted at non-textured at the current cutting conditions. The perpendicular and the parallel texture can change the chip flow angle at 44 and 90°, respectively. The rectangular texture does not show any alteration in chip flow angle. Simulation results showed that the chip flow angle can be governed from 116 to 44° via edge distance. Pitch size can play the chip flow angle between 26 and 30°, whereas the texture height can play between 35 and 44° at the considered range of the texture parameters. The friction factor can vary the chip flow angle between 44 and 52°. A compact control on the chip flow angle can help in designing the chip breaker and chip removal from the machining zone effectively.

Acknowledgments This research was partly supported by the Human Resource Training Project for Regional Innovation funded by National Research Foundation (NRF) of Korea (No. 2012H1B8A2026133) and development of nano-based ultraprecision hybrid machining system technology, funded by the Ministry of Trade, Industry & Energy (MOTIE) of Korea.

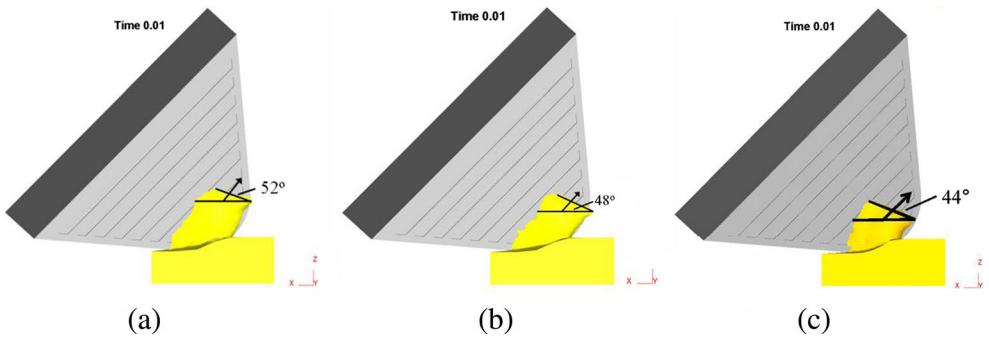

Fig. 15 Effect of friction force on the chip flow angle at **a** 0.2, **b** 0.4, and **c** 0.6

References

1. Huang Y, Chou YK, Liang S (2007) CBN tool wear in hard turning: a survey on research progresses. Int J Adv Manuf Technol 35(5–6): 443–453. doi:10.1007/s00170-006-0737-6
2. Konig W, Berktold A, Koch KF (1984) Machining of hard materials, vol 2. CIRP, Annals of
3. Zhang J (2005) Process Optimization for Machining of hardend Steels. Ph. D. Thesis, Georgia Institute of Technology
4. Dawson TG (2002) Machining hardened steel with polycrystalline cubic boron nitride cutting tools. Ph.D. Thesis, Georgia Institute of Technology,
5. Al-Zkeri IA (2007) Finite element modeling of hard turning. Ph. D. Thesis, Ohio State University
6. Ramesh A, Melkote SN, Allard LF, Riester L, Watkins TR (2005) Analysis of white layers formed in hard turning of AISI 52100 steel. Mater Sci Eng A 390(1–2):88–97. doi:10.1016/j.msea.2004.08.052
7. Bruzzone AAG, Costa HL, Lonardo PM, Lucca DA (2008) Advances in engineered surfaces for functional performance. CIRP Ann Manuf Technol 57(2):750–769. doi:10.1016/j.cirp.2008.09.003
8. Evans CJ, Bryan JB (1999) "Structured", "Textured" or "Engineered" surfaces. CIRP Ann Manuf Technol 48(2):541–556. doi:10.1016/s0007-8506(07)63233-8
9. Kawasegi N, Sugimori H, Morimoto H, Morita N, Hori I (2009) Development of cutting tools with microscale and nanoscale textures to improve frictional behavior. Precis Eng 33(3):248–254. doi:10.1016/j.precisioneng.2008.07.005
10. Lian Y, Deng J, Yan G, Cheng H, Zhao J (2013) Preparation of tungsten disulfide (WS2) soft-coated nano-textured self-lubricating tool and its cutting performance. Int J Adv Manuf Technol 68(9–12): 2033–2042. doi:10.1007/s00170-013-4827-y
11. Pettersson U, Jacobson S (2006) Tribological texturing of steel surfaces with a novel diamond embossing tool technique. Tribol Int 39(7):695–700. doi:10.1016/j.triboint.2005.06.004
12. Dubrujeaud B, Vardavoulias M, Jeandin M (1994) The role of porosity in the dry sliding wear of a sintered ferrous alloy. Wear 174(1–2):155–161. doi:10.1016/0043-1648(94)90097-3
13. Blatter A, Maillat M, Pimenov SM, Shafeev GA, Simakin AV, Loubnin EN (1999) Lubricated sliding performance of laser-patterned sapphire. Wear 232(2):226–230. doi:10.1016/S0043-1648(99)00150-7
14. Costa H, Hutchings I (2009) Effects of die surface patterning on lubrication in strip drawing. J Mater Process Technol 209(3):1175–1180
15. Erdemir A (2005) Review of engineered tribological interfaces for improved boundary lubrication. Tribol Int 38(3):249–256. doi:10.1016/j.triboint.2004.08.008
16. Xie J, Luo MJ, Wu KK, Yang LF, Li DH (2013) Experimental study on cutting temperature and cutting force in dry turning of titanium alloy using a non-coated micro-grooved tool. Int J Mach Tools Manuf 73:25–36. doi:10.1016/j.ijmachtools.2013.05.006
17. Tatsumi T, Takeda J, Imai K, Hashimoto H (1999) An engineered tool and some results of fly-cut experiments. Precision Engineering, Nanotechnology, Vol 1, Proceedings. Shaker Verlag Gmbh, Aachen
18. Hintze W. EA, and Wurfels K. (1998) Tool for material removal machining. US Patent
19. Jianxin D, Ze W, Yunsong L, Ting Q, Jie C (2012) Performance of carbide tools with textured rake-face filled with solid lubricants in dry cutting processes. Int J Refract Met Hard Mater 30(1):164–172. doi:10.1016/j.ijrmhm.2011.08.002
20. Johnson GR, Cook WH A constitutive model and data for metals subjected to large strains, high strain rates and high temperatures. In: Proceedings of the 7th International Symposium on Ballistics (1983) The Hague. International Ballistics Committee, Netherlands, pp 541–547
21. Tang L, Huang J, Xie L (2011) Finite element modeling and simulation in dry hard orthogonal cutting AISI D2 tool steel with CBN cutting tool. Int J Adv Manuf Technol 53(9–12):1167–1181. doi:10.1007/s00170-010-2901-2
22. Obikawa T, Kamio A, Takaoka H, Osada A (2011) Micro-texture at the coated tool face for high performance cutting. Int J Mach Tools Manuf 51(12):966–972. doi:10.1016/j.ijmachtools.2011.08.013
23. Huang Y, Liang S (2003) Cutting forces modeling considering the effect of tool thermal property—application to CBN hard turning. Int J Mach Tools Manuf 43(3):307–315
24. Guo Y, Liu C (2002) 3D FEA modeling of hard turning. J Manuf Sci Eng 124(2):189–199
25. Umbrello D, Hua J, Shivpuri R (2004) Hardness-based flow stress and fracture models for numerical simulation of hard machining AISI 52100 bearing steel. Mater Sci Eng A 374(1):90–100
26. Ng EG, Aspinwall DK, Brazil D, Monaghan J (1999) Modelling of temperature and forces when orthogonally machining hardened steel. Int J Mach Tools Manuf 39(6):885–903. doi:10.1016/s0890-6955(98)00077-7
27. Heath P (1987) Properties and uses of Amborite. Carbide Tool J 19(2):12–14